JOURNAL OF MATERIALS SCIENCE 39 (2004) 1389– 1395

Using ESPI system to measure high temperature fatigue deformation of ceramics thermally sprayed SUS304 steel

R. WANG*
Mechanical System Engineering, Graduate School of Engineering, Hiroshima University, 1-4-1 Kagamiyama, Higashi-Hiroshima 739-8527, Japan
E-mail: wangrg2003@hotmail.com

M. KIDO
Department of Mechanical System Engineering, Hiroshima Institute of Technology, Saeki-ku, Hiroshima 731-5193, Japan

The strains in an Al_2O_3/NiCr coating, which was thermally sprayed on SUS304 steel, were analyzed using an electronic speckle pattern interferometry (ESPI) system during fatigue testing ($R = 0$, $\sigma_{max} = 173$ MPa) at high temperature of 873 K. The strain changes with the crack initiation in the coatings and the delamination at the coating/substrate interface are accordingly discussed.

Surface cracks originated from the top coating of Al_2O_3 and stopped at the bond coating of NiCr after 2 cycles test at 873 K. Many surface cracks and delamination along the NiCr/substrate interface were confirmed after 1×10^5 cycles test. The strain values of un-sprayed specimens obtained from the ESPI system agreed with those measured by the strain gauge when tensile stresses were applied at room temperature. The deformation by thermal expansion and stress application at high temperatures can also be easily measured using this method. The strain on sprayed specimens was almost the same with that on un-sprayed specimens at 873 K, indicating the deformation in the coatings are always associated with that of the substrate surfaces at high temperature. By comparing and analyzing the strain distribution on the coating surface, the presence of cracks in the coatings and delamination at the coating/substrate interface can be *in-situ* and nondestructively detected.

1. Introduction

Thermally spraying ceramic coatings are usually used as thermal barrier coatings (TBC) because of their high thermal resistance [1]. However, their integrity and reliability might be compromised when the deformation becomes large. Although much research [2–16] on damage behavior of ceramic coatings have been carried out, there are few reports [3–6] on their deformation/damage behaviors at high temperature because it is difficult to apply the strain gauge method at high temperature. Particularly there is almost no research on the nondestructive detection of crack initiation and delamination of thermally sprayed coatings at high temperature. In order to solve these problems, non-contact measuring methods are necessary.

The electronic speckle pattern interferometry (ESPI) [17–20] method is one of the effective ways to measure deformation without contacting the specimen. Although this method has been successfully applied at room temperature, its application at high temperature has not been well studied. Okura *et al.* [3–6] measured the fatigue strain within an area of diameter ϕ 1 mm on a ceramic sprayed material at high temperature using a SSDG (Speckle Strain/Displacement Gauge) method similar to the ESPI method, in which a laser beam of diameter ϕ 1 mm was illuminated to specimen surfaces and the reflected laser lights from two directions were detected. On the other hand, the ESPI method used in this work had two laser lights illuminating the specimen surfaces and the deformation within a large area of about 200 mm $\times$ 300 mm can be simultaneously measured.

In this work, fatigue tests were carried out on an Al_2O_3/NiCr sprayed onto SUS304 stainless steel, and the surface deformation/damage behaviors were investigated using the ESPI method. The relations between surface deformation and crack/delamination of coatings are discussed.

2. Experimental details

Solution treated SUS304 steel (C: 0.06%, Si: 1.00%, Mn: 2.00%, P: 0.045%, S: 0.030%, Cr: 18.00%, Ni:

*Author to whom all correspondence should be addressed.

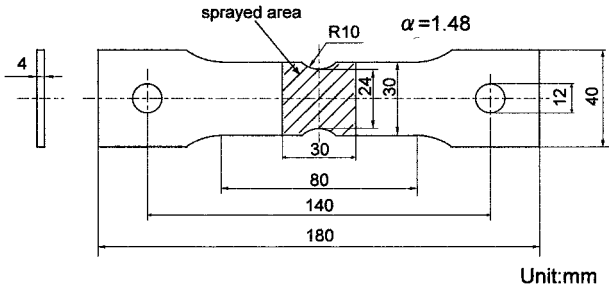

Figure 1 Specimen shape used in test.

8.00%, $\sigma_{0.2} = 290$ MPa) was used as the substrate. The specimen shape is shown in Fig. 1. The atmospheric plasma spraying apparatus (TECHNOSERVE CO., LTD) was used to spray Al_2O_3(outer top coating)/Ni80%Cr20% (inner bond coating) coating on the hatching area shown in Fig. 1. The spraying conditions are shown in Table I.

Fatigue tests were carried out with a servo pulse fatigue-testing machine (Shimadzu Co.: EHF-EG50KN-20L) at 873 K. The stress ratio (R) was 0, the nominal stress (σ_{max}: at the specimen center) was 173 MPa, the frequency (f) was 6.7 Hz, and the load was sinusoidally controlled. The fatigue test was paused after a certain number of test cycles, and then surface speckles were recorded with the ESPI system (Dr. ETTEMEYER GmbH & Co., Q-300) when step-by-step nominal tensile stresses (increment: 10.4MPa) were loaded (unloaded) in the order of 0 MPa $\rightarrow$ 173 MPa $\rightarrow$ 0 MPa. All the stress values in the following description are nominal tensile stresses.

The schematic illustration of the ESPI system is shown in Figs 2 and 3. Two illuminated laser lights produce a speckle (Fig. 2b) on the specimen surface. The speckle moves (changes) when deformation occurs on the specimen surface. Correlation fringes (Fig. 3b) can be produced when speckles before and after deformation are interfered. The displacement (u) (Fig. 3c) of specimen surface is given by Equation 1 [18, 19].

$$u = \frac{n\lambda}{2\sin\frac{\theta}{2}}. \quad (1)$$

where n is the number of the fringe, λ is the laser wave length (750 nm), θ is the angle between the two illuminated laser beams. The strain distribution (Fig. 3d) can

TABLE I Plasma spraying conditions

	Al_2O_3 ceramics coating	Ni–Cr coating
Chemical composition (wt%)	99.8% Al_2O_3	80%Ni, 20%CR
Grain size (μm)	20.7	70.8
Arc current (A)	450	400
Arc voltage (V)	45	30
Gas		
Ar (mm^3/s)	2.5×10^5	3.3×10^5
He (mm^3/s)	8.3×10^4	–
Spraying distance (mm)	100	100
Coating thickness (μm)	100 ± 20	100 ± 20

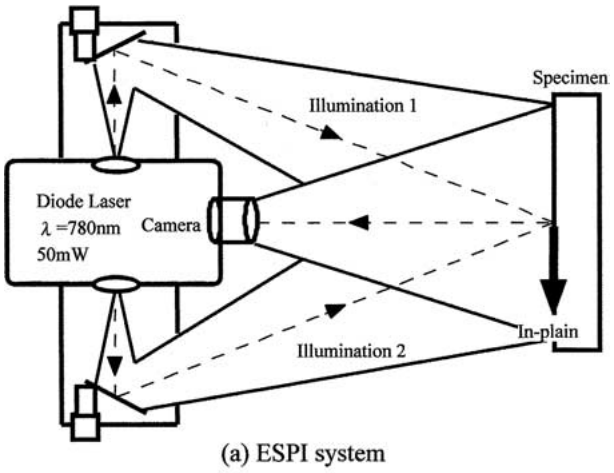

(a) ESPI system

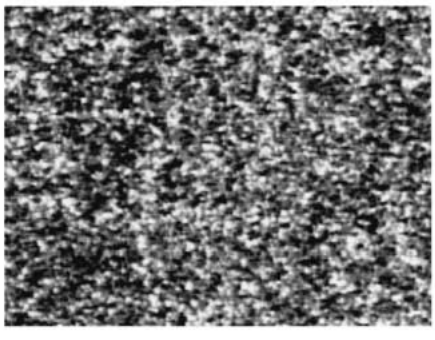

(b) Typical speckle pattern

Figure 2 (a) Schematic illustration of electronic speckle pattern interferometry (ESPI) system and (b) typical speckle pattern.

be obtained by differentiating the displacement distribution (Fig. 3c). The color variation from black, blue to red on displacement/strain distribution figures means the displacement/strain value increase. The calibration length to calculate strains was 0.2 mm in this work.

The ESPI system (type Q-300, Dr. ETTEMEYER GmbH & Co.) was used, by which a minimum displacement of 0.03 μm can be detected. The deformation measurement areas in this work were the same with spraying areas at room temperature and the 24 mm $\times$ 5 mm center area (Fig. 3a) at high temperature, respectively. Left side and right side as shown in Fig. 3a had two gradual waists (hereinafter, called notches). Data processes were carried out using the ISTRA data system (Dr. ETTEMEYER GmbH & Co.).

The surface and cross-section morphologies before and after fatigue tests were observed with scanning electron microscope (SEM). Specimens were heated with an induction heating system and the temperature was measured with a radiation thermometer.

3. Results and discussion

3.1. Strain values by strain gauge and ESPI method

Fig. 4 shows strain values by strain gauge and ESPI method (calibration length: 5 mm) at the same position E and C on the un-sprayed specimen at room temperature. This result indicates good correspondence of strain values by strain gauge and ESPI method.

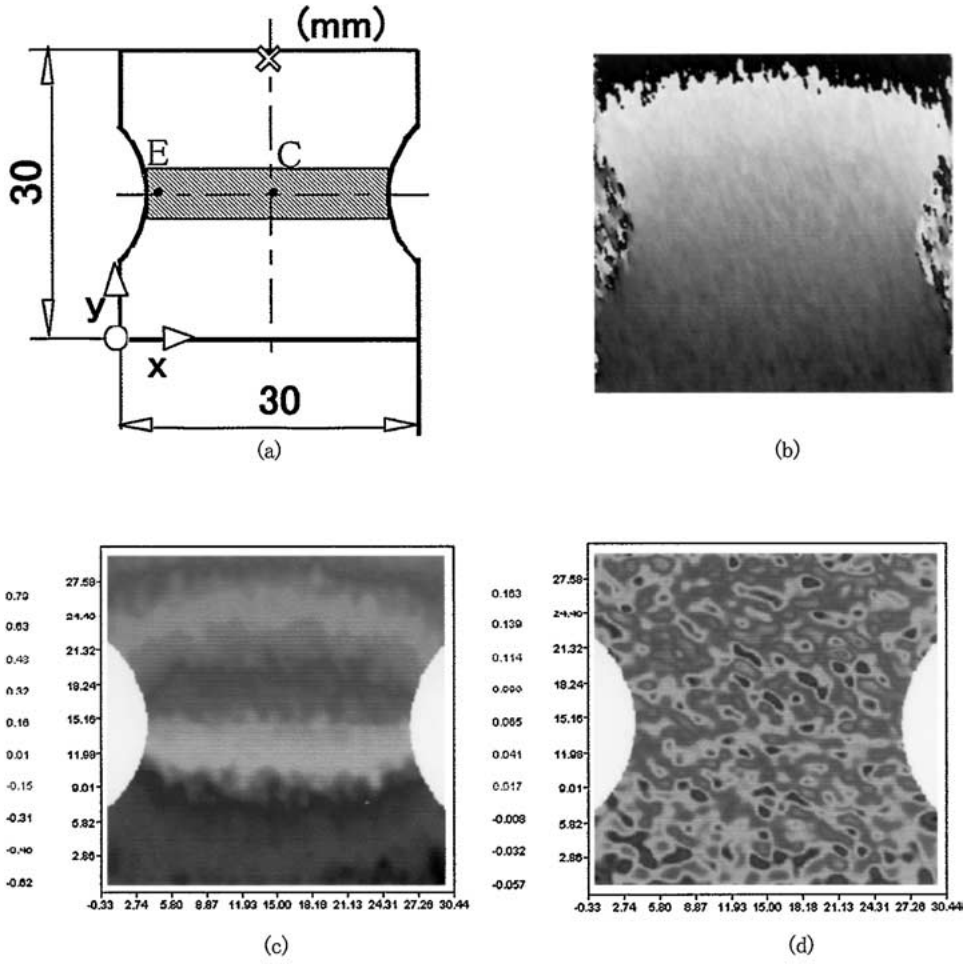

Figure 3 The measurement coordinate (a), interferometry fringe phase distribution (b), displacement distribution (c) and strain distribution (d) of SUS304 steel specimen when a nominal tensile stress is loaded to 10.4 MPa at 293 K.

3.2. Deformation measurement by ESPI method at high temperature

Fig. 5 shows the strain values of un-sprayed and sprayed specimens, which were heated to 873 K, loaded to 173 MPa and held for 15 ks. The strain changes for both specimens due to heat were much larger than those due to load and creep.

Fig. 6 shows the typical strain values at centers of un-sprayed and sprayed specimens at $N = 2$ and 1×10^5 cycle. The maximum strain values were almost the same for both specimens. However, the deformation at $N = 2$ cycle was a little larger than that at $N = 1 \times 10^5$ cycle. Generally, the Young's moduli of thin Al_2O_3 and NiCr spraying coatings are much lower than their bulk values due to porosity [10]. Their Young's moduli are also much lower than the SUS304 steel substrate [3]. Accordingly, the restriction effect of the coatings on the substrate deformation was small and thus the deformation of the thin coatings would be almost the same as the

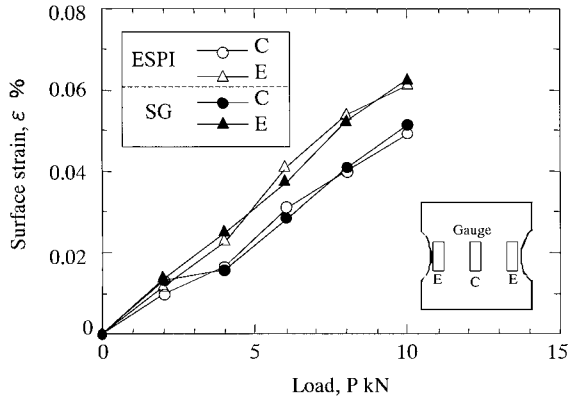

Figure 4 Load-strain curves (gauge length: 5 mm) according to strain gauge (SG) and ESPI system.

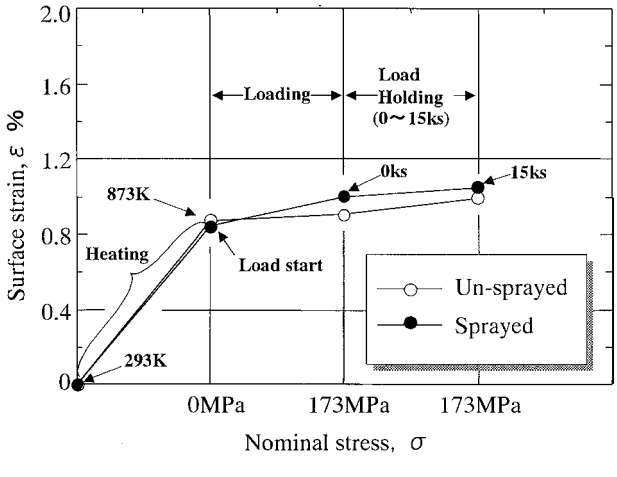

Figure 5 Strain variations measured at the center of un-sprayed and sprayed specimens with the process of heating (293–873 K), loading (nominal stress 0–173 MPa) and holding (0–15 ks).

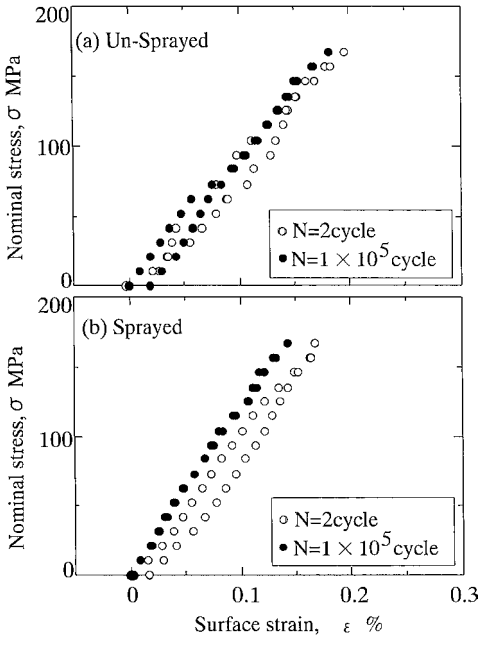

Figure 6 Nominal stress-strain curves measured at the center of unsprayed and sprayed specimen at 873 K.

uncoated substrate. The Vickers hardness (9.8 N, 15 s) was measured at center and near (1 mm) notch root of substrate before and after 1×10^5 cycles tests at 873 K. The hardness before test was $HV = 226$, and that after 1×10^5 cycles at 873 K this became $HV = 237$ (center) and $HV = 260$ (near notch root), indicating that the deformation decrease after 1×10^5 cycles test at 873 K was resulted from the work hardening effect of austenite steel under cyclic stress.

3.3. SEM observation of sprayed specimens before and after fatigue tests

Fig. 7 shows surface and cross-section (near notch root) morphologies of sprayed specimens after 2 and 1×10^5 cycles fatigue test. Surface cracks had initiated from the notch root on the Al_2O_3 outer coating and then stopped at the NiCr inner coating after 2 cycle test. Although no cracks were observed in substrate, delamination along the NiCr/substrate interface was confirmed and surface cracks propagated through the NiCr coating after 1×10^5 cycles test. Cracks and delamination were also observed at the center of the specimen. There were no cracks or delamination observed at $\sigma_{max} = 140$ MPa after 2 cycles and $\sigma_{max} = 108$ MPa after 1×10^5 cycles.

3.4. Cracks and delamination detection by ESPI method

The stress-strain curves measured at two positions of A and B at $N = 1$ cycle test are shown in Fig. 8a. The strains linearly increased with stress increase initially until suddenly becoming much larger when $\sigma = 125$ MPa. According to SEM observation after 1×10^5 cycles (Fig. 8b), separately occurred were observed at position A and B, indicating these cracks were not propagated from cracks near notch root but from inner defects in coating. The sudden strain increase can be attributed to the sudden initiation/opening of cracks and then their combination [21]. Positions of cracks occurring during loading might be identified using this method. Moreover, the residual strain of about 0.25% was due to the residual opening of cracks.

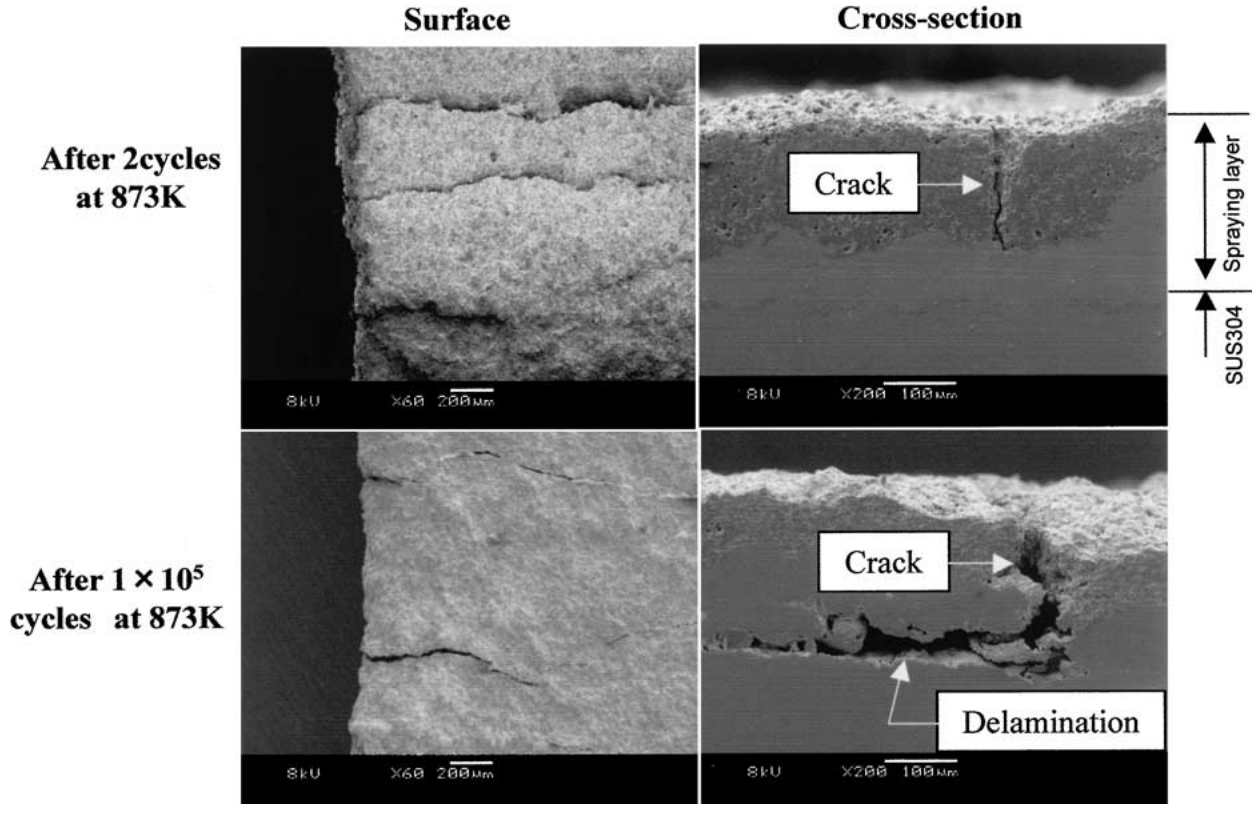

Figure 7 Surfaces and cross-section morphologies near the notch of sprayed specimen after fatigue test at 873 K.

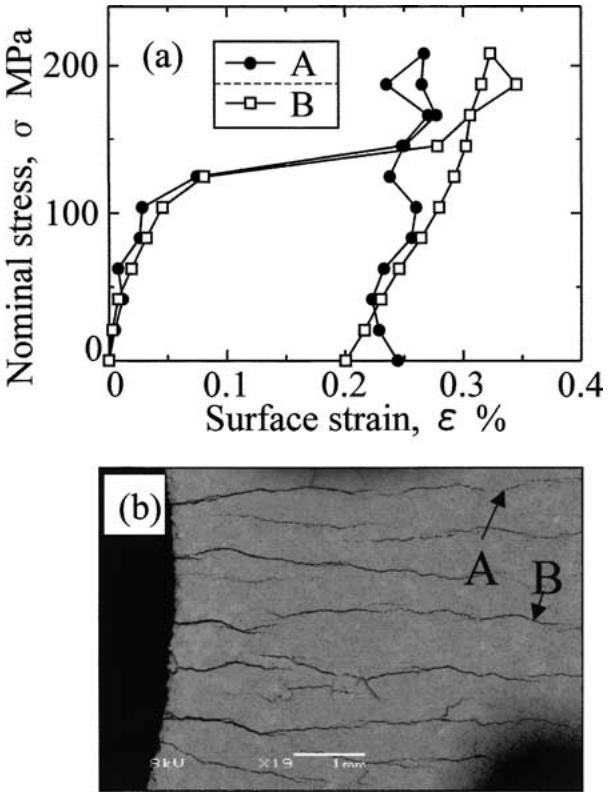

Figure 8 The stress-strain curves (a) at the positions A and B (b, c, d) of a sprayed specimen where crack initiation occurred not form the notch root when a nominal stress of 173 MPa was applied at 873 K.

The identification of cracks using the strain increase phenomenon on surfaces is discussed in the following. Fig. 9a and b show the displacement and strain distributions on the sprayed specimen surface with long cracks (>5 mm) when a nominal stress 104 MPa was loaded. These cracks occurred in condition ($\sigma_{max} = 208$ MPa, $T = 873$ K) for 1 cycle test. With comparing the strain concentration zones (red zones) positions in Fig. 9a and b and cracks positions in Fig. 9c, their correspondence was clear, i.e., cracks larger than 5 mm can be detected by using the ESPI method.

Fig. 10 shows one result of the displacement and strain distributions ($N = 1 \times 10^5$ cycle) and surface/cross-section morphologies after 1×10^5 cycles test. The strain concentration zones on the left side corresponding to crack positions (Fig. c1 and c2), while cracks cannot be confirmed on the right side (Fig. d1, Al_2O_3 side: A.S). However, cracks (Fig. d2 and d3) in Ni-Cr layer were observed and correspond to the strain concentration zones positions on the right NiCr side (N.S) after delaminated the coating with quick cooling. Accordingly, short cracks as 500 μm and inner cracks could be also detected using the ESPI method. It is clear that the appearance of higher strain values along the crack (Figs 9b and 10b) was originated from the large change of the displacement near the crack (Figs 9a and 10a), which would be attributed to the crack opening when applying a tensile stress.

Fig. 11 shows another result of the strain distribution at $N = 1$ cycle (a), $N = 2$ cycle (b) and $N = 1 \times 10^5$ cycle (c) and surface (d) (e) (f) and cross-section (g) morphologies after 1×10^5 cycles test. Although the deformation was unstable during the initial load, it became stable and strain concentration zones appeared near notch root from $N = 2$ cylce test. However, the strain decrease at position A with increasing cycles was clear. Their stress-strain curves measured by ESPI at position A (Fig. 11a) is shown in Fig. 12. Although a

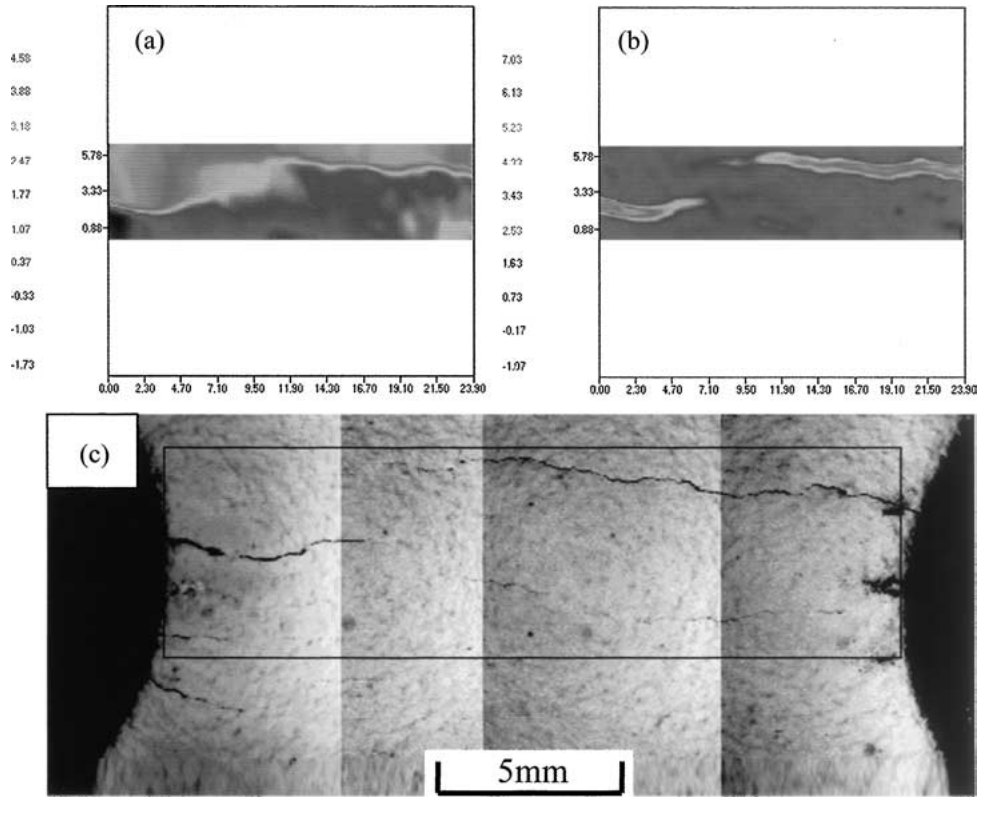

Figure 9 The distribution of displacement (a) and strain (b) on a sprayed specimen surface (c) with long cracks when a nominal stress of 104 MPa was applied at 873 K.

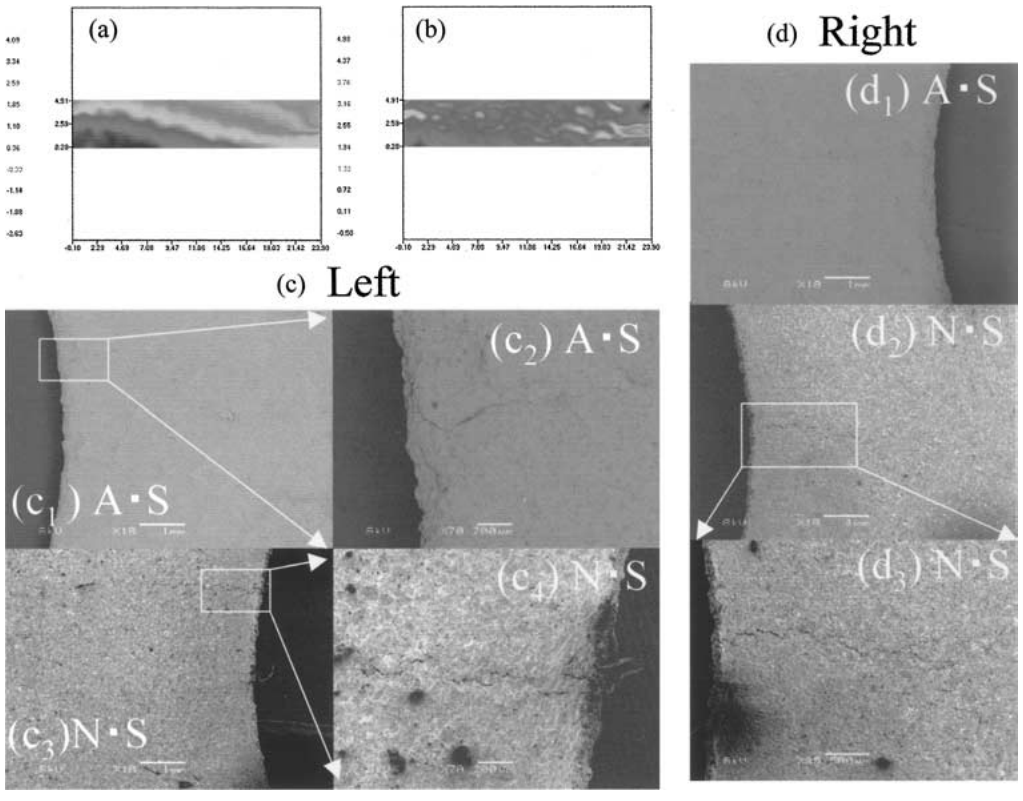

Figure 10 The distribution of displacement (a) and strain (b) on a sprayed specimen surface, where no cracks exist on the right Al_2O_3 side (d1), but small cracks exist on left Al_2O_3 side (c1, c2) and Ni-Cr side (c3, c4) and right Ni-Cr side (d2, d3) of the spraying film while, when a nominal stress of 173 MPa was loaded at 873 K.

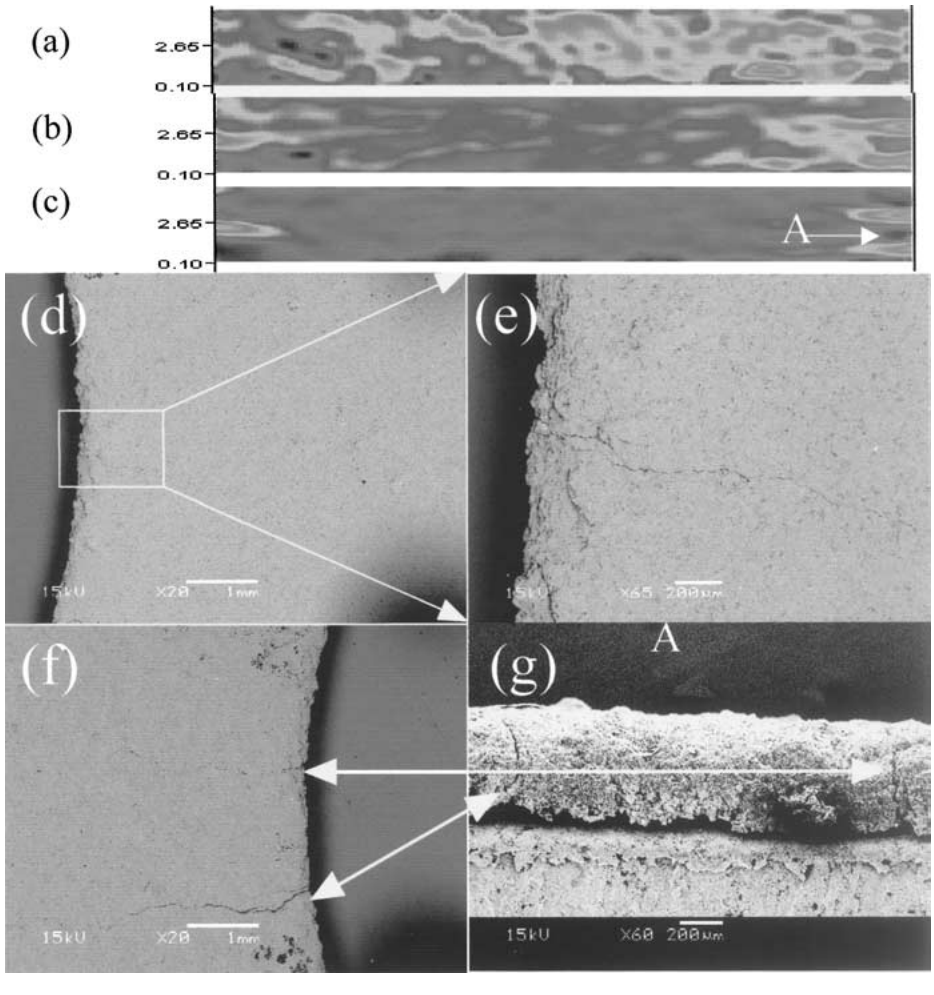

Figure 11 The correspondence of strain concentration (a) 1cycle, (b) 2cycles, (c) 1 $\times 10^5$ cycles) and cracks (d, e) left side surface; (f) right side surface, (g) right side cross-section) on a sprayed film when a nominal stress of 173 MPa was loaded at 873 K.

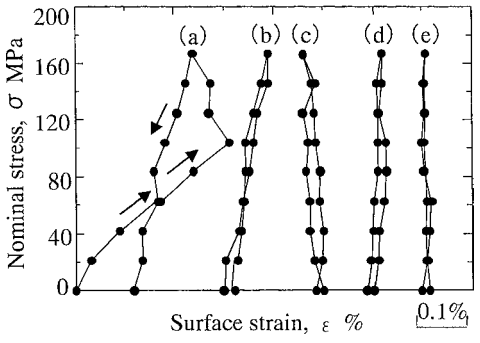

Figure 12 The stress-strain curves measured at the position A in Fig. 11 with the increase of fatigue cycles: (a) $N = 1$ cycle, (b) $N = 2$ cycle, (c) $N = 100$ cycle, (d) $N = 1 \times 10^4$ cycle and (e) $N = 1 \times 10^5$ cycle.

maximum strain of about 0.25% occurred at $N = 1$ cycle, it decreased from $N = 100$ cycle. On the other hand, local delamination after 1×10^5 cycles test was confirmed near position A (Fig. 11f and g). Generally, when delamination (near a crack) occurs between the coating and the substrate, the deformation of the delaminated part will not be constricted by the substrate, i.e., the stress from the substrate interface would not be correctly transmitted to the coating. Thus, the deformation there would be much smaller than that not delaminated when a tensile stress was applied, which is the reason why we considered the large decrease of surface strain with cycles in point C was due to the local delamination of the spraying coating from the substrate.

According to the above results, the initiation and existence of cracks/delamination in sprayed coatings during fatigue testing can be non-destructively detected by analyzing strain concentration or decrease using the ESPI method. In further work, other spraying materials and composites will be applied to confirm the applicability of ESPI method further. Moreover, more studies of high temperature fatigue deformation of sprayed materials under various stress conditions are planned in order to make the best use of the ESPI method for detection of cracks and delamination of sprayed materials.

4. Conclusions

Fatigue tests were carried out on Al_2O_3/NiCr thermally sprayed onto SUS304 steels at 873 K. The influence of cracks and delamination on surface deformation was investigated by electronic speckle pattern interferometry (ESPI) method. The following results were obtained.

(1) The strain values measured by the ESPI method agree with those measured by strain gauge at room temperature.

(2) The surface deformation was almost the same for un-sprayed and sprayed specimens, indicating that the deformations of the coatings was controlled by the substrate. The maximum strain at $N = 1 \times 10^5$ cycle was slightly smaller than that at $N = 2$ cycle.

(3) Cracks in the Al_2O_3 coating had occurred but stopped at NiCr coating after 2 cycles fatigue test when σ_{max} was 173 MPa at 873 K ($R = 0$). Cracks propagated through NiCr coating and caused delamination along the NiCr/substrate interface after 1×10^5 cycle tests.

(4) The strain concentration and the strain decrease on the coating surface with cyclic stress measured by ESPI method can be used to detect the crack initiation in coatings and the delamination occurrence at the coating/substrate interface.

References

1. K. KOJIMA, *J. Surf. Finish. Soc. Jpn.* **41** (1990) 988.
2. M. KIDO, R. WANG, S. NAKAMURA, M. TAKEDA, M. YAMAZAKI and T. TOKUDA, *J. Soc. Mater. Sci. Jpn.* **51** (2002) 1417.
3. I. NISHIKAWA, K. OGURA, M. YAMAGAMI and K. KUWAYAMA, *ibid.* **43** (1994) 1290.
4. H. WAKI, K. OGURA and I. NISHIKAWA, *JSME Intern. J.* Series A **44** (2001) 374.
5. 5H. WAKI, M. NISHII, K. OGURA and I. NISHIKAWA, *ibid.* **66** (2000) 1520.
6. H. WAKI, K. OGURA, I. NISHIKAWA, H. NAGAMURA and M. NISHII, *ibid.* **66** (2001) 1148.
7. A. IBRAHIM and C. C. BERNDT, *J. Mater. Sci.* **33** (1998) 3095.
8. Y. ITOH, M. SATOH, Y. HARADA and J. TAKEUCHI, *J. Soc. Mater. Sci. Jpn.* **44** (1995) 1361.
9. M. TAKEDA, T. OKABE, M. KIDO and Y. HARADA, *J. Jpn. Therm. Spray. Soc.* **38** (2001) 58.
10. T. SHIRAISHI, H. OGIYAMA, H. TSUKUDA and Y. SOYAMA, *J. Hig. Tem. Soc.* **17** (1991) 34.
11. 11T. OGAWA, *J. Jpn. Therm. Spray. Soc.* **35** (1998) 307.
12. M. OHKI, T. HWU, Y. MUTOH, H. KITA and Y. UNNO, *ibid.* **36** (1999) 12.
13. J. OH, J. KOMOTORI and M. SHIMIZU, *ibid.* **37** (2000) 166.
14. J. HWANG, T. OGAWA, K. TOKAJI, T. EJIMA, Y. HOBAYASHI and Y. HARADA, *J. Soc. Mater. Sci. Jpn.* **45** (1996) 927.
15. H. SUZUKI, T. UEKI and M. FUKUMAOTO, *Trans. Jpn. Soc. Mech. Eng.* Series A **57** (1991) 1062.
16. D. ZHANG, M. KATO and K. NAKASA, *J. Soc. Mater. Sci. Jpn.* **48** (1999) 1065.
17. A. J. MOORE and J. R. TYRER, *J. Strain Analysis* **29** (1994) 257.
18. S. TOYOOKA, *Mater. Techn.* **70** (2000) 869.
19. K. KIM and M. MUROZONO, *Trans. Jpn. Soc. Mech. Eng,* Series A **60** (1994) 2567.
20. S. DILHAIRE, S. JOREZ, A. CORNET, E. SCHAUB and W. CLAEYS, *Microelectr Reliab.* **39** (1999) 981.
21. T. TORII, K. HONDA, T. FUJIBAYASHI and T. HATANO, *Trans. Jpn. Soc. Mech. Eng.* Series A **55** (1989) 1525.

Received 16 May 2002
and accepted 4 September 2003